FEBS Letters 589 (2015) 718–725

FEBS Letters

journal homepage: www.FEBSLetters.org

Redox-dependent translocation of the heat shock transcription factor AtHSFA8 from the cytosol to the nucleus in *Arabidopsis thaliana*

Miriam Giesguth [1], Arne Sahm [1], Swen Simon [1], Karl-Josef Dietz *

Biochemistry and Physiology of Plants, Bielefeld University, 33615 Bielefeld, Germany

ARTICLE INFO

Article history:
Received 30 November 2014
Revised 29 January 2015
Accepted 29 January 2015
Available online 7 February 2015

Edited by Julian Schroeder

Keywords:
AtHSFA8
Fluorescence resonance energy transfer
Heat stress transcription factor
Redox-regulation
Cytoplasmic-nuclear shuttling
Reactive oxygen species

ABSTRACT

The hypothesis is tested that some heat stress transcription factors (HSFs) are activated after formation of inter- or intramolecular disulfide bonds. Based on in silico analyses we identified conserved cysteinyl residues in AtHSFA8 that might function as redox sensors in plants. AtHSFA8 represents a redox-sensitive transcription factor since upon treatment of protoplasts with H_2O_2 YFP-labeled HSFA8 was translocated to the nucleus in a time-dependent manner. Site-directed mutagenesis of the conserved residues Cys24 and Cys269 blocked translocation of HSFA8 to the nucleus. The findings concur with a model where HSFA8 functions as redox sensing transcription factor within the stress-responsive transcriptional network.

1. Introduction

A major increase above growing temperature poses an environmental challenge to sustained plant fitness. The heat shock response (HSR) system is highly conserved among all cells. This system includes transcription factors which activate protective genes. Heat stress leads to accumulation of reactive oxygen species (ROS) [1] which alter redox homeostasis and oxidize cell constituents. Volkov et al. [2] observed that ROS, especially H_2O_2, are needed to activate the HSR. Mittler et al. [3] suggested that also other ROS including singlet oxygen ($^1O_2$), superoxide anion ($O_2^{\cdot-}$) and hydroxyl radical ($HO^{\cdot}$) may play a role. Normally ROS are rapidly detoxified by scavenging mechanisms including superoxide dismutase, ascorbate peroxidase, peroxiredoxin and glutathione peroxidase [4,5]. On the other hand ROS are needed to activate signal transduction pathways and mediate appropriate acclimation responses [6,7]. Based on the widely assumed model for the HSR in plants [6,8,9], HSFs are kept inactive in the cytosol by interaction with heat shock proteins (HSPs) masking the nuclear location signal (NLS) and the oligomerisation domain. When stress triggers an imbalance in cellular protein homeostasis, HSPs are recruited to act as chaperones, HSFs oligomerize and translocate to the nucleus where they activate the expression of target genes. Following a mostly unknown deactivation mechanism, HSFs are translocated back to the cytosol, bind to HSPs and return to their inactive state.

HSFs display a modular structure and recognize palindromic binding motifs, the so called heat shock elements (HSE; 5′-AGA-AnnTTCT-3′) in the promoter region of stress-inducible genes [10]. The highly conserved DNA-binding domain (DBD) is located at the N-terminus. The oligomerisation domain (HR-A/B region) is connected to the DBD by a variable linker. This region is involved in the formation of the coiled-coil structure of the HSF oligomers.

HSFs form a complex network that responds to several abiotic stresses and involves different cellular compartments [7]. H_2O_2 plays a key role in plants as a signaling molecule [11]. There exists a link between the HSR and the ROS response [12]. Miller and Mittler [3] suggested that some oxidative stress-responsive HSFs such as HSFA2, HSFA4a and HSFA8 act as H_2O_2-sensors similar to mammalian and *Drosophila* HSFs [13]. But the mechanism used

Abbreviations: CFP, cyan fluorescent protein; CLSM, confocal laser scanning microscopy; DBD, DNA-binding domain; DCF, dichlorofluorescein; DCFH-DA, 2′,7′-dichlorofluorescein diacetate; DTT, dithiothreitol; FRET, fluorescence resonance energy transfer; HSE, heat shock element; HSF, heat stress transcription factor; HSP, heat shock protein; HSR, heat shock response; NES, nuclear export signal; NLS, nuclear localization signal; OD, HR-A/B region or oligomerisation domain; ROS, reactive oxygen species; WT, wild type; YFP, yellow fluorescent protein.

* Corresponding author at: Biochemistry and Physiology of Plants, W5-134, Bielefeld University, University Str. 25, 33501 Bielefeld, Germany. Fax: +49 521 1066039.
E-mail address: karl-josef.dietz@uni-bielefeld.de (K.-J. Dietz).
[1] Fax: +49 521 1066039.

http://dx.doi.org/10.1016/j.febslet.2015.01.039
0014-5793/

to recognize and sense H_2O_2 in the cytosol is still elusive. The transcription factors may be sensitive to H_2O_2 using 'single-Cys' or 'two-Cys' redox sensory mechanisms [14]. Redox sensors often are constituted of specific accessible cysteines that exist as thiolate anions ($-S^-$) and have enhanced reactivity to ROS [15]. They reversibly switch between an oxidized state with inter- or intramolecular disulfide bonds and a reduced state. Such thiol-disulfide transitions are often involved in redox-regulation in plants [16].

Our work aimed at identifying and studying conserved cysteine residues in HSFs, which could act as redox sensors and might be involved in regulation of the redox- and ROS-dependent responses. An alignment of homologous HSFs allowed for identifying highly conserved Cys in HSFA8. Protoplasts transiently co-transfected with GFP:HSF fusion-constructs were subjected to oxidative or reductive conditions. HSFA8 was translocated from the cytosol to the nucleus upon H_2O_2 treatment. The significance of specific Cys residues could be shown using the mutant variants HSFA8C24S or HSFA8C269S which showed no translocation to the nucleus upon oxidative stress. These results link subcellular localization of HSF to redox milieu and specific Cys residues and provide new insights in the *Arabidopsis thaliana* heat stress transcription factor network.

2. Materials and methods

2.1. Plant growth

A. thaliana ecotype Col-0 was grown on the MPI-soil mixture (MPIPZ, Cologne Project 187509, Germany) supplemented with Osmocote Start fertilizer (Scotts, USA) and Lizetan (Bayer, Germany) in a growth chamber with constant humidity of 55% and a day/night cycle of 10/14 h with quantum flux density of about 100 μmol quanta m^{-2} s^{-1}.

2.2. Isolation, staining and transfection of protoplasts

A. thaliana mesophyll protoplasts were prepared according to Seidel et al. [17,18]. Transfection of about 1000 protoplasts was performed with 75 μg plasmid DNA for each construct. H_2O_2 and DTT were added at concentrations as indicated and image analysis was performed with AxioVision LE4.3 (Zeiss, Göttingen, Germany). For heat treatment, the protoplast-containing Petri dishes were placed in a water bath at 40 °C for given time [18]. The use of Leptomycin B (LMB) as an inhibitor for the nuclear export [19] was performed with 30 nM and the protoplasts were incubated for 3 h until analysis. The subcellular localization was visualized on the single cell level after 2 h with a confocal laser scanning microscope (Leica SP2, Heidelberg, Germany). Unstressed samples served as control for each experiment. For the quantification of the oxidative stress effects of H_2O_2 the protoplasts were loaded with 5 μM 2′,7′-dichlorofluorescein diacetate (DCFH-DA, Sigma–Aldrich, Hamburg, Germany) by incubating them in W5-solution containing DCFH-DA. Afterwards the protoplasts were washed twice. These protoplasts were treated with increasing concentrations of H_2O_2 from 0 to 10 mM for 30, 60 or 90 min. The fluorescence emission of DCF and the chlorophyll autofluorescence were monitored with an AxioSkop 2 microscope using filter 09 (Zeiss, Göttingen, Germany). Pictures were taken with the AxioCam IC c1 (Zeiss, Göttingen, Germany). The intensities of green DCF emission and red autofluorescence were estimated with GIMP 2.6 (GNU Image Manipulation Program; Free Software Foundation, USA) and the green-to-red ratio was calculated.

2.3. Molecular cloning

Full-length cDNA sequence of HSFA8 (At1g67970) and HSC70-1 (At5g02500) were obtained from the TIGR database (http://www.tigr.org). The open reading frame was amplified from *A. thaliana* cDNA without the stop codon using gene-specific primer pairs introducing flanking restriction sites for BamHI and AgeI in HSFA8 and BamHI in HSC70-1. All amplified products and the vectors 35S-YFP-NosT and 35S-CFP-NosT [18] were digested with the restriction enzymes BamHI and AgeI (NEB) and purified (Promega, Wizard_Plus DNA purification kit). All constructs were sequenced.

The mutants HSFA8C24S, HSFA8C269S or the double mutant HSFA8C24SC269S were generated with mutagenesis PCR using primers with single nucleotide exchanges (Suppl. Table S1, [20]).

2.4. Analysis of in vivo interaction by FRET

To perform FRET measurements 35S-HSFA8:YFP/35S-HSFA8:CFP were co-transfected into *A. thaliana* mesophyll protoplasts. All given combinations were analyzed using a confocal laser scanning microscope (Leica SP2, Heidelberg, Germany). FRET measurements were done, microscope settings selected and FRET efficiencies calculated as described before [17,18,21].

2.5. Bioinformatic analysis

Gene models of HSFs of *A. thaliana* were retrieved from the Plant Transcription Factor DataBase (Pln TFDB; [22]) and blasted for homologous sequences of HSFs. Following multiple alignments of the 15 coding sequences with highest similarity, the conserved Cys residues were identified and phylogenetic trees automatically constructed using a custom-built program written in YAVA script. A major element of the program was the determination of a score which describes the degree of conservation of the Cys residues and comparing it with the likelihood that a Cys at the same position originated by coincidence (Supplementary material). Subcellular localization of AtHSFA8 was predicted with www.cbs.dtu.dk/services/SignalP/ and www.bar.utoronto.ca/interactions/cgi-bin/arabidopsis_interactions_viewer.cgi. For determination of three dimensional structure of AtHSFA8 the RCSB Protein Database (www.rcsb.org) was used together with SWISS-MODEL (swissmodel.expasy.org/) and the visualization tool chimera (www.cgl.ucsf.edu/chimera/). The intramolecular disulfide formation of the two cysteines in HSFA8 was predicted with http://clavius.bc.edu/~clotelab/DiANNA) [23].

3. Results and discussion

Gene models of the HSF family members were sorted according their conserved cysteines with the highest conservation score (Table 1). Based on the top scoring position in the list and the previous suggestion as potentially redox sensitive HSF [3], respectively, HSFA1a and HSFA8 were selected for biochemical confirmation. Subsequent analyses showed that HSFA1a localized to the nucleus under all test conditions and therefore was not further analyzed (data not shown). For HSFA8 the best 15 hits based on overall sequence identity were selected and a phylogenetic tree was calculated. The tree topology was colored separately for each cysteine of the gene model to depict the conservation status of the cysteine among the different homologues (Suppl. Fig. 1). The tree topology of HSFA8 is shown with the coloring of the putative redox-active cysteine (Cys24). Fig. 1 shows the alignment region in vicinity of the redox-active cysteines of HSFA8. The alignments enabled us to determine the conservation status of each cysteine of the gene models in regard to the homologues. In case of HSFA8, 5 out of the 15 most similar sequences contained the Cys. Putative HSFA8 homologues were identified in papaya, grape and poplar. Among the conserved cysteines (Fig. 1 and Table 1) which might be involved in sensing changes in the redox milieu of the cell by

Table 1
Overview of all 25 gene models encoding HSFs form *A. thaliana* sorted by their cysteines with the highest conservation score. Marked in red is the transcription factor AtHSFA8, which was studied further.

At number	Name	Sequence length (AA)	Quantity of Cys	Best conserved Cys	Score of best conserved Cys
AT4G17750.1	HSFA1a	496	1	1	0.733
AT3G22830.1	HSFA6b	407	1	1	0.6
AT4G11660.1	HSFB2b	378	5	3	0.533
AT1G32330.1	HSFA1d	486	2	1	0.467
AT2G26150.1	HSFA2	346	2	1	0.4
AT1G67970.1	HSFA8	375	2	1	0.333
AT1G46264.1	HSFB4	349	2	1	0.333
AT5G45710.1	HSFA4c	346	2	2	0.267
AT5G16820.1	HSFA1b	482	3	1	0.267
AT5G16820.2	HSFA1b	482	3	1	0.267
AT2G41690.1	HSFB3	245	5	5	0.267
AT4G18880.1	HSFA4a	402	6	3	0.2
AT3G02990.1	HSFA1e	469	5	2	0.2
AT4G36990.1	HSFB1	285	4	3	0.133
AT5G62020.1	HSFB2a	300	3	2	0.133
AT5G43840.1	HSFA6a	283	4	2	0.067
AT5G54070.1	HSFA9	332	4	1	0.067
AT5G03720.1	HSFA3	413	3	1	0.067
AT4G13980.1	HSFA5	467	2	1	0.067
AT3G51910.1	HSFA7a	273	2	1	0
AT2G26150.2	HSFA2	291	3	1	0
AT3G24520.1	HSFC1	331	1	1	0
AT1G77570.1	–	148	2	1	0
AT4G18870.1	–	292	3	1	0
AT3G63350.1	HSFA7b	283	0	–	–

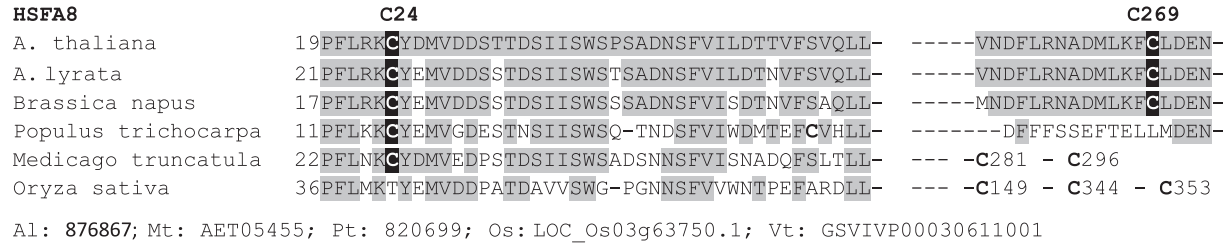

Fig. 1. Partial alignment of AtHSFA8 and related HSFs. Conserved cysteines in the sequence are marked black. The grey boxed amino acid residues are identical to AtHSFA8. The homologue to C24 in HSFA8 is found in selected HSF variants from dicotyledoneous plants. The homologue to C269 is only found in *Brassicaceae*. There exists the possibility that Cys at different positions could substitute for C269 in other dicotyledoneous HSFs.

reversible thiol modifications [15], Cys24 is conserved in dicots, whereas Cys269 only occurred in Brassicaceae (*Arabidopsis lyrata*, *Brassica napus*, *Eutrema salsugineum*). In *Medicago truncatula* as in other dicots alternative Cys-residues exist downstream of the second Cys in AtHSFA8. For AtHSFA8, Cys24 in the DNA-binding domain and Cys269 in the C-terminal part of the protein were considered as promising candidates for redox regulation by intramolecular disulfide formation.

Localization studies of HSFA8 were performed as follow up to the in silico analyses (Suppl. Fig. 2) and revealed a cytosolic location. In the next step it was explored whether an oxidative stress or heat stimulus might affect HSFA8 localization. Under oxidising conditions imposed by H_2O_2-treatment (Fig. 2B) HSFA8 moved from the cytosol to the nucleus within 2 h. HSFA8 was neither partitioned from the cytosol to the nucleus upon DTT-treatment nor in the untreated control (Fig. 2A and C). Interestingly, heat stress of 40 °C (Fig. 2E) was also ineffective. According to Mittler et al. [14] HSFs could sense the H_2O_2-content inside the cell with "single-Cys" or "two-Cys" mechanisms by reversible thiol modifications. Our work addressed this hypothesis by determining the subcellular localization of HSFA8 under conditions of oxidative stress. To quantify the oxidising effect of externally applied H_2O_2, a quantification of DCF fluorescence in *A. thaliana* protoplasts in the presence of different H_2O_2 concentrations was performed (Fig. 3). DCF fluorescence increased with rising H_2O_2 concentrations (Fig. 3A). The fluorescence intensity increased in two phases, a sensitive rise below 2 mM H_2O_2 and a steady rise at higher H_2O_2. Signal intensity was high after 30 min and slightly decreased at 60 min, and further at 90 min (Fig. 3B). The latter may indicate processes such as decomposition of H_2O_2, degradation of the fluorescent dye or activated defence reactions of the cells. As shown before [2,24] *A. thaliana* cell cultures have a high capacity to reduce exogenous H_2O_2, but it seems likely that enough H_2O_2 was outside to modify the redox state of the cytosol and to shift the redox state of the thiol-/disulfide redox regulatory network to a more oxidising state [25,26]. Thus thiol oxidation appears to trigger the translocation of HSFA8. Little is known about the threshold, time delay and concentration of H_2O_2 needed to activate HSFA8 translocation. This may explain why heat stress despite its effect on cell ROS development was unable to initiate HSFA8 translocation to the nucleus. Interestingly Miller and Mittler failed to observe transcriptional regulation of HSFA8 after heat shock [3]. These results for the time being characterize HSFA8 as redox-sensitive but not heat-responsive HSF.

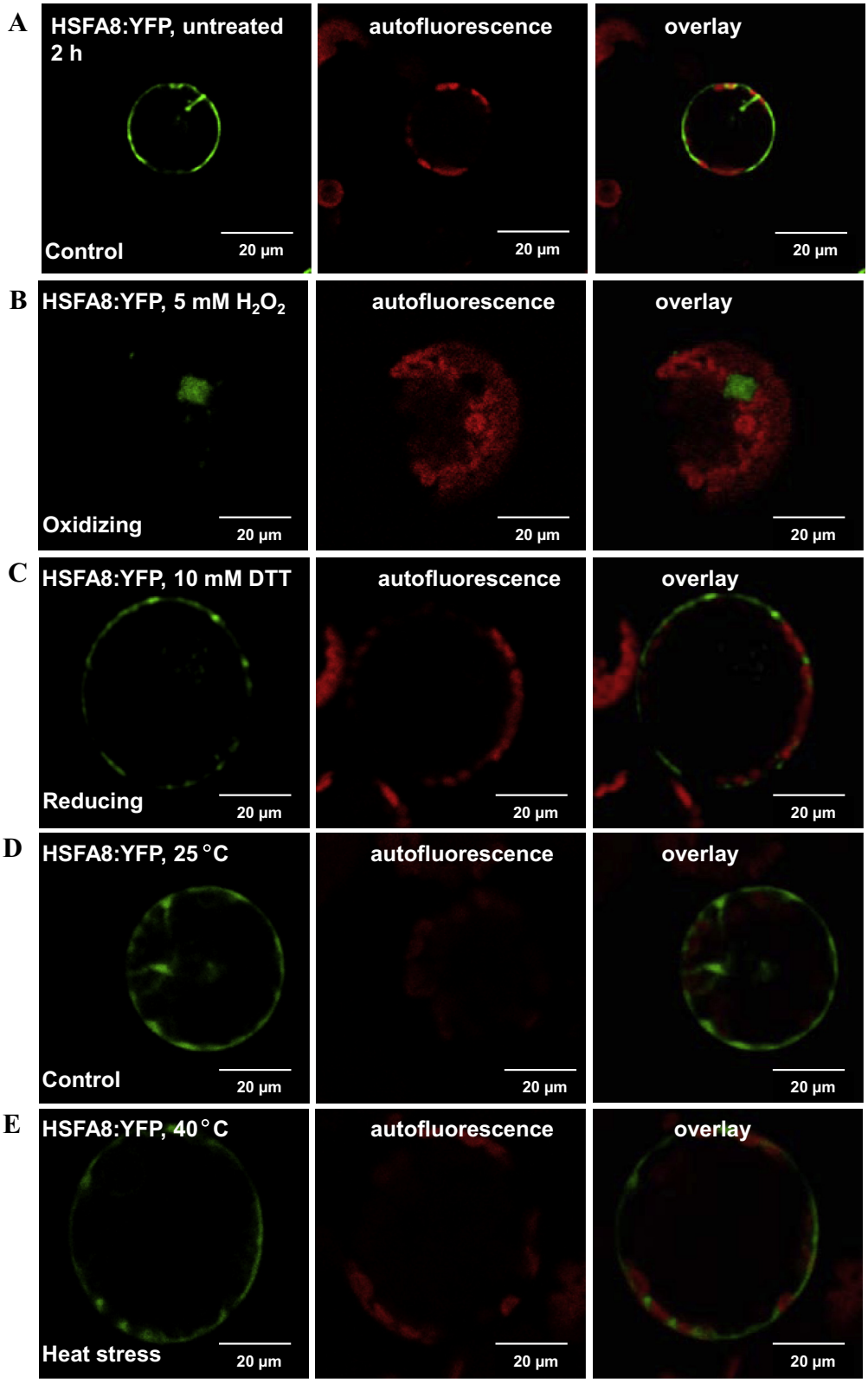

Fig. 2. Time-dependent translocation of HSFA8:YFP in protoplasts under different treatments. Localization of HSFA8:YFP was recorded under control (A), oxidising (5 mM H_2O_2) (B), and reducing conditions (10 mM DTT) (C). The images on the left hand side show YFP-fluorescence as green signal, in the middle the autofluorescence in red, and on the right hand side the overlay of all. Protoplasts were transfected with 75 µg DNA of HSFA8:YFP. H_2O_2 or DTT were added at t = 16 h after transfection. Images were taken after 2 h. Under oxidising conditions HSFA8:YFP showed nuclear localization, while HSFA8:YFP was located in the cytosol under reducing conditions. This type of localization was seen in many transfected protoplasts. Localization of HSFA8:YFP in transfected *A. thaliana* protoplasts following a heat treatment at 40 °C (E) in comparison to the control treatment at 25 °C (D). The color coding and the time points are the same as described above.

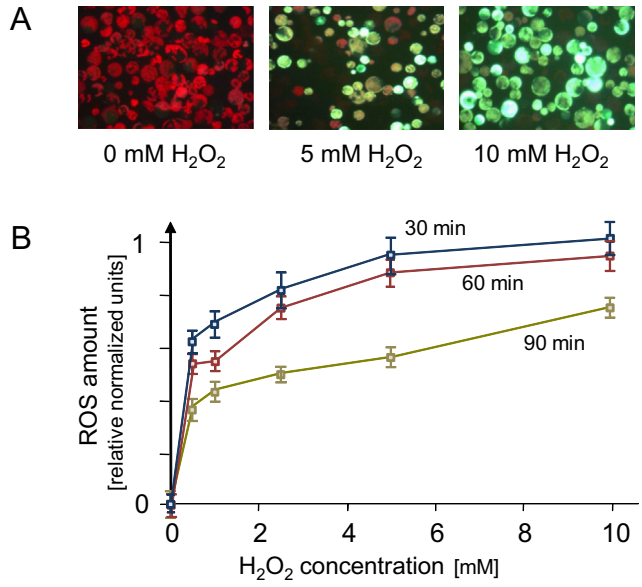

Fig. 3. Quantification of DCF fluorescence in *A. thaliana* protoplasts under different H_2O_2 concentrations. (A) Representative images of *A. thaliana* protoplasts showing oxidative stress-induced green fluorescence emitted from 2′,7′-dichlorofluorescein (DCF) under increasing H_2O_2 concentrations. The increasing H_2O_2 concentration correlates with the accumulation of green fluorescence. (B) Concentration-dependent increase of DCF-fluorescence in protoplasts at different H_2O_2 concentrations. The green emission of the DCF and the red autofluorescence were evaluated with GIMP 2.6 and the ratio between green and red intensities plotted against increasing H_2O_2 concentrations. The background in the absence of H_2O_2 treatment was subtracted and the maximal fluorescence value was set to 1. Signals were evaluated in three different experiments. Data are means ± S.E., $n = 48$.

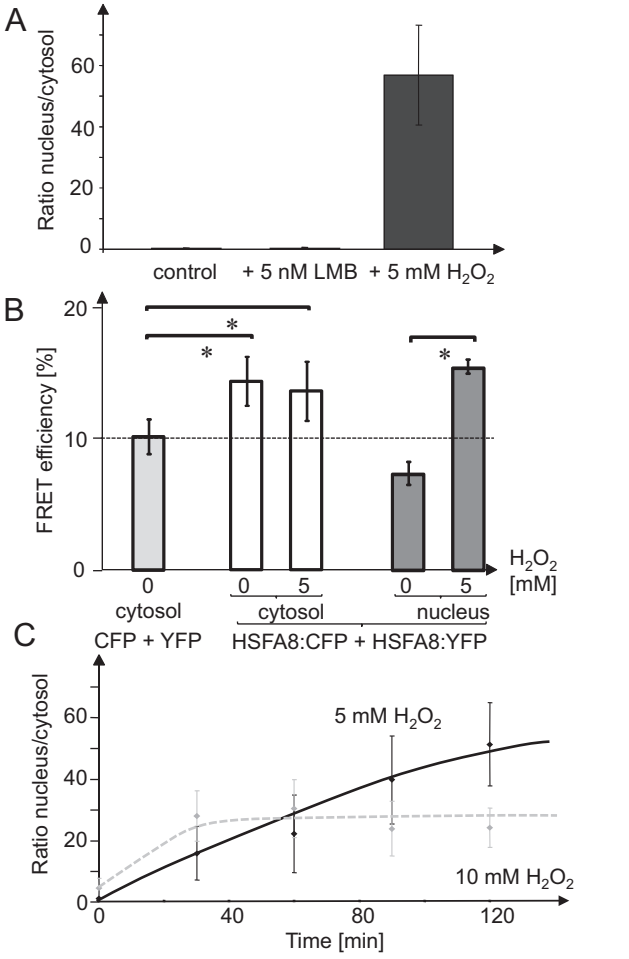

Fig. 4. Effect of Leptomycin B on translocation, HSFA8 oligomerisation, and time dependent translocation. (A) LMB was added to HSFA8:YFP-transfected protoplasts at $t = 16$ h and compared with untreated controls. Also shown is the efficient translocation upon H_2O_2 treatment. YFP fluorescence was quantified in representative virtual transects of the cytosol and the nucleus after 2 h (cf. Suppl. Fig. 3) and intensity ratios calculated. Data are means ± S.E., $n = 10$. (B) Oligomerisation of HSFA8 following H_2O_2-treatment studied by FRET. Protoplasts were co-transfected with HSFA8:CFP and HSFA8:YFP. The fluorophores were fused to the C-terminal end of HSFA8 in both constructs. HSFA8 was located in the cytosol and only conditionally translocated to the nucleus. The fluorescence in the cells was measured before and after addition of H_2O_2 (5 mM, 90 min). The FRET threshold was obtained from control transfections with P_{35S}-CFP and P_{35S}-YFP. FRET efficiency was calculated according to [21]. *Indicates significance at $p < 0.05$ in Student's t-test. Data are means ± S.E., $n = 95$ protoplasts. (C) Time-dependent translocation of HSFA8:YFP from cytosol to nucleus. Protoplasts were transfected with HSFA8:YFP. H_2O_2 was added to the protoplast suspension at $t = 16$ h. The value of the cytosol was set to unity and the value in the nucleus expressed as fold value of cytosol. Data are means ± S.E., $n = 15$.

In the next step we wanted to address the possibility that HSFA8 continuously shuttles between cytosol and nucleus. In this scenario oxidative inhibition of export eventually caused by H_2O_2 could allow for nuclear accumulation. Protoplast samples were supplemented with Leptomycin B (LMB) which inhibits nuclear export [19] (Fig. 4A). Permanent shuttling and oxidative inhibition of export can be excluded since LMB caused no accumulation of HSFA8 in the nucleus. Activation of HSFs is suggested to involve oligomerisation. Therefore, the translocation of HSFA8:YFP upon initiation of oxidative stress was further investigated by exploring oligomerization by in vivo FRET analysis (Fig. 4B). The FRET efficiency between fused YFP and CFP indicative for HSFA8 protein–protein interaction was calculated according to [21]. As shown in Fig. 4B, the FRET efficiency in the nucleus increased significantly from 6.4 ± 0.8% which is below the significance threshold of interaction to 15.9 ± 0.5% after adding H_2O_2 to the protoplasts. The corresponding data of the cytosol were 14.4 ± 1.9% at 0 mM H_2O_2 and 13.6 ± 2.3 at 5 mM H_2O_2 treatment. Both values showed a significant difference to the FRET-control measurement with free (unfused) CFP and YFP. The nuclear HSFA8 revealed no interaction at all in the 0 mM H_2O_2 treatment which may be caused by the extremely low concentration of HSFA8 in the nucleus of untreated cells. Unchanged FRET efficiency between HSFA8:CFP and HSFA8:YFP in the cytosol contradicts the hypothesis of trimerisation as prerequisite for activation (Fig. 4). Chan-Schaminet et al. [27] reported that HSF oligomers already exist in the cytoplasm of tomato under unstressed conditions. HSFA8 oligomers pre-exist in the cytosol as seen in Fig. 4. The quantitative analysis of the nucleus-localized YFP fluorescence revealed a significant increase of HSFA8 oligomers in the nucleus after applying 5 mM H_2O_2 to the cells. This discovery was further explored in dependence on time by quantifying the movement in transfected protoplasts with HSFA8:YFP (Fig. 4C). The emission intensity of YFP-fluorescence was quantified along a half transect across the protoplast image or in the nuclear region of interest (ROI) (Suppl. Fig. 3). To get a measure for the HSFA8 translocation, the maximal nuclear intensity was divided by the maximal intensity in the cytosol at the time points as indicated. These ratios were plotted against the exposure time to H_2O_2 (Fig. 4C). A significant rise in the intensity ratio between nucleus and cytosol upon H_2O_2 treatment was observed between $t = 0$ h until 2.5 h. The intensity versus time curve at lower H_2O_2 increased roughly linearly with a trend to slow saturation. In contrast, the treatment with 10 mM H_2O_2 caused a rapid rise within the first 30 min and then stayed at a rather constant level. The initial rise was close to twice as fast as in the case of 5 mM H_2O_2 and the difference to the pretreatment value was already significant at $t = 30'$. These results indicate conformational changes of

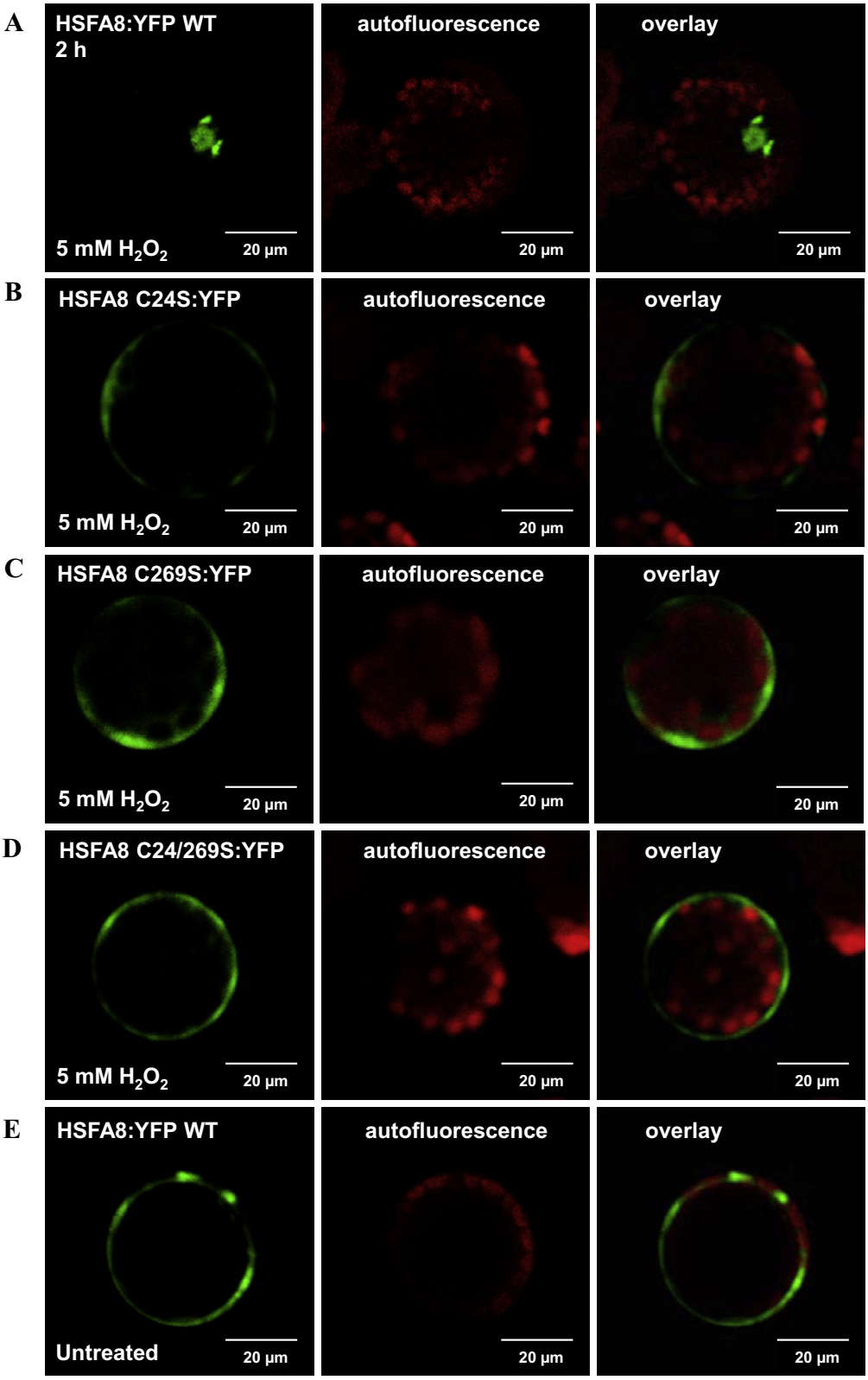

Fig. 5. Images of *A. thaliana* protoplasts transfected with HSFA8:YFP WT or HSFA8 cysteine mutants under oxidising conditions. Protoplasts were transfected with HSFA8:YFP WT (A) and subsequently treated with 5 mM H_2O_2. Same experiment was performed with HSFA8 C24S:YFP (B), and HSFA8 C269S:YFP (C) or double mutant HSFA8 C24/269S:YFP (D). The wild type HSFA8 image without treatment is given in (E). Protoplasts were transfected with 75 µg DNA of the corresponding constructs. H_2O_2 at 5 mM concentration was added at t = 16 h after transfection. Images were recorded after 2 h. Under oxidising conditions HSFA8:YFP showed the nuclear localization. In a converse manner HSFA8 C24S:YFP, HSFA8 C269S:YFP and HSFA8 C24/269S retained their cytosolic localization and lacked the translocation to the nucleus. The same images were recorded in 9 protoplasts (A–C) and 5 protoplasts (D, E), respectively.

HSFA8 in vivo. To gain a better insight into how HSFA8 might sense the hydrogen peroxide in the cytosol a putative homology model was generated with a protein structure prediction tool (Suppl. Fig. 4A). The model shows the typical modular structure of HSFs [10]. For HSFA8 a putative disulfide bond formation between Cys_{24} and Cys_{269} was predicted (Suppl. Fig. 4B) which would likely cause a drastic conformational change and might induce the translocation to the nucleus.

To challenge this hypothesis, variants of HSFA8 namely C24S, C269S and the double mutant HSFA8 C24/269S were generated to test, if the two cysteines in HSFA8 are required for the translocation from the cytosol to the nucleus under oxidising conditions. Protoplasts were transfected with the described constructs (Fig. 5), and the intracellular distribution of the fusion proteins was monitored under oxidising conditions after 2 h. As shown before, HSFA8:YFP WT moved from the cytosol to the nucleus. In a converse manner the single mutants HSFA8 C24S (Fig. 5B) and HSFA8 C269S (Fig. 5C), and the double mutant HSFA8 C24/269S (Fig. 5D) remained in the cytosol and did not show any accumulation in the nucleus within 2 h.

The widely accepted model of HSR [6,8,9] assumes that HSFs bind to HSPs under non-stress conditions. Interaction partners of HSFA8 were searched in silico with the interaction viewer, and the heat shock protein HSC70 was predicted to interact with HSFA8. Based on this information and the common HSR model, HSC70 was cloned in an expression vector and cotransfected with HSFA8-fluorophore fusion constructs into protoplasts (Fig. 6). In these experiments, FRET efficiency between HSFA8:YFP and HSFA8-CFP reached values of about 24.1% and thus exceeded that shown in Fig. 4. Coexpression of unlabeled HSC70 did not change this high value since the trend to increased FRET was insignificant. Subsequently, HSC70:YFP and HSFA8:CFP and the swapped fluorophores were tested for interaction between HSC70 and HSFA8 FRET efficiencies of 21.6 ± 4.2% and 25.6 ± 3.1% demonstrated molecular interaction in the cytosol to confirm the predicted interaction. FRET-values in the nucleus were significantly lower. It will be interesting to investigate the effect of oxidative treatment on HSC70/HSFA8 interaction in the cytosol in order to advance the mechanistic model.

Apparently, the redox-sensing mechanism of HSFA8 was linked to the presence of Cys_{24} and Cys_{269}. Deletion of either single Cys or both abolished ROS-induced accumulation of HSFA8 in the nucleus. The results are in line with the assumption that disulfide bond formation between Cys_{24} and Cys_{269} controls the partitioning of HSFA8 between the cytosol and the nucleus. Another possibility could be the formation of intramolecular disulfide bridges stabilizing the DNA binding (Cys_{24}) on the one hand, and the transcriptionally active module in the CTD (C_{269}) on the other hand. Several testable explanations may be proposed: One explanation could be the unmasking of the nuclear import sequence upon disulfide bridge formation. Alternatively, oxidation could mask the export signal (NES) [28]. Thirdly, oxidised HSFA8 might be released from multi-heteromeric complexes as proposed for the heat-induced activation of HSF. The large intervening amino acid sequence between Cys_{24} and Cys_{269} suggests that disulfide bond formation causes profound conformational changes which probably are required for the translocation to the nucleus [29]. HSC70, a homologue of the HSP70 family interacted with HSFA8 in the cytosol. Analysis of the dynamics of this interaction in vitro and in vivo may provide further clues on involved structural dynamics. In conclusion, our work demonstrates the function of HSFA8 as redox-sensor, which is able to recognize oxidising conditions in the cytosol of a single cell and is subsequently translocated to the nucleus. This sensor may also be used in future experiments to monitor ROS and redox signaling in single cells. The regulatory features of other HSFs should be investigated for their responsiveness to H_2O_2 similar to the analysis presented here [30].

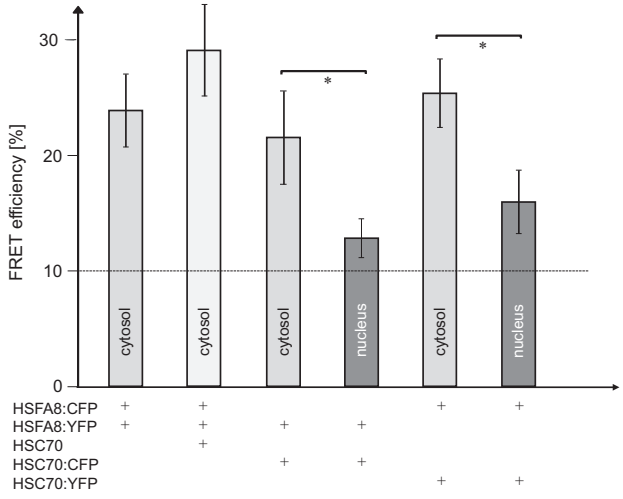

Fig. 6. Interaction between HSC70 and HSFA8 in vivo. Protoplasts were transfected with the constructs as indicated. FRET was quantified. The effect of co-expressed unlabelled HSC70 on HSFA8:CFP/HSFA8:YFP interaction was also tested (second column). Data are means ± S.E. of $n = 36$ (first two columns) and $n = 25$ (third to sixth columns). Asterisks mark significance of difference between FRET efficiencies in cytosol and nucleus, $p < 0.05$ (Student's t-test).

Acknowledgments

We are very grateful to Dr. Klaus-Dieter Scharf (Goethe-Universität Frankfurt) for valuable advice. This work was founded by the DFG, by research efforts within the SFB613, project D12, and Di 346 (SPP1710).

Appendix A. Supplementary data

Supplementary data associated with this article can be found, in the online version, at http://dx.doi.org/10.1016/j.febslet.2015.01.039.

References

[1] Vacca, R.A., de Pinto, M.C., Valenti, D., Passarella, S., Marra, E. and de Gara, L. (2004) Production of reactive oxygen species, alteration of cytosolic ascorbate peroxidase, and impairment of mitochondrial metabolism are early events in heat shock-induced programmed cell death in tobacco Bright-Yellow 2 cells. Plant Physiol. 134, 1100–1112.
[2] Volkov, R.A., Panchuk, I.I., Mullineaux, P.M. and Schoffl, F. (2006) Heat stress-induced H(2)O(2) is required for effective expression of heat shock genes in Arabidopsis. Plant Mol. Biol. 61, 733–746.
[3] Miller, G. and Mittler, R. (2006) Could heat shock transcription factors function as hydrogen peroxide sensors in plants? Ann. Bot. 98, 279–288.
[4] Dietz, K.J. (2008) Redox signal integration: from stimulus to networks and genes. Physiol. Plant. 133, 459–468.
[5] Oelze, M.L., Kandlbinder, A. and Dietz, K.J. (2008) Redox regulation and overreduction control in the photosynthesizing cell: complexity in redox regulatory networks. Biochim. Biophys. Acta 1780, 1261–1272.
[6] Mittler, R., Finka, A. and Goloubinoff, P. (2012) How do plants feel the heat? Trends Biochem. Sci. 37, 118–125.
[7] Qu, A.L., Ding, Y.F., Jiang, Q. and Zhu, C. (2013) Molecular mechanisms of the plant heat stress response. Biochem. Biophys. Res. Commun. 432, 203–207.
[8] Hahn, A., Bublak, D., Schleiff, E. and Scharf, K.D. (2011) Crosstalk between Hsp90 and Hsp70 chaperones and heat stress transcription factors in tomato. Plant Cell 23, 741–755.
[9] Scharf, K.D., Berberich, T., Ebersberger, I. and Nover, L. (2012) The plant heat stress transcription factor (Hsf) family: structure, function and evolution. Biochim. Biophys. Acta 1819, 104–119.
[10] Nover, L., Bharti, K., Doring, P., Mishra, S.K., Ganguli, A. and Scharf, K.D. (2001) Arabidopsis and the heat stress transcription factor world: how many heat stress transcription factors do we need? Cell Stress Chaperones 6, 177–189.
[11] Vranova, E., Inze, D. and van Breusegem, F. (2002) Signal transduction during oxidative stress. J. Exp. Bot. 53, 1227–1236.

[12] Suzuki, N. and Mittler, R. (2006) Reactive oxygen species and temperature stresses: a delicate balance between signaling and destruction. Physiol. Plant. 126, 45–51.
[13] Ahn, S.G. and Thiele, D.J. (2003) Redox regulation of mammalian heat shock factor 1 is essential for Hsp gene activation and protection from stress. Genes Dev. 17, 516–528.
[14] Mittler, R., Vanderauwera, S., Suzuki, N., Miller, G., Tognetti, V.B., Vandepoele, K., et al. (2011) ROS signaling: the new wave? Trends Plant Sci. 16, 300–309.
[15] Zaffagnini, M., Bedhomme, M., Marchand, C.H., Morisse, S., Trost, P. and Lemaire, S.D. (2012) Redox regulation in photosynthetic organisms: focus on glutathionylation. Antioxid. Redox Signal. 16, 567–586.
[16] Bykova, N.V. and Rampitsch, C. (2013) Modulating protein function through reversible oxidation: redox-mediated processes in plants revealed through proteomics. Proteomics 13, 579–596.
[17] Seidel, T., Kluge, C., Hanitzsch, M., Ross, J., Sauer, M., Dietz, K.J. and Golldack, D. (2004) Colocalization and FRET-analysis of subunits c and a of the vacuolar H+-ATPase in living plant cells. J. Biotechnol. 112, 165–175.
[18] Seidel, T., Golldack, D. and Dietz, K.J. (2005) Mapping of C-termini of V-ATPase subunits by in vivo-FRET measurements. FEBS Lett. 579, 4374–4382.
[19] Kudo, N., Wolff, B., Sekimoto, T., Schreiner, E.P., Yoneda, Y., Yanagida, M., et al. (1998) Leptomycin B inhibition of signal-mediated nuclear export by direct binding to CRM1. Exp. Cell Res. 242, 540–547.
[20] König, J., Galliardt, H., Jütte, P., Schäper, S., Dittmann, L. and Dietz, K.J. (2013) The conformational bases for the two functionalities of 2-cysteine peroxiredoxins as peroxidase and chaperone. J. Exp. Bot. 64, 3483–3497.
[21] Schnitzer, D., Seidel, T., Sander, T., Golldack, D. and Dietz, K.J. (2011) The cellular energization state affects peripheral stalk stability of plant vacuolar H+-ATPase and impairs vacuolar acidification. Plant Cell Physiol. 52, 946–956.
[22] Riaño-Pachón, D., Ruzicic, S., Dreyer, I. and Mueller-Roeber, B. (2007) PlnTFDB: an integrative plant transcription factor database. BMC Bioinformatics 8, 42.
[23] Ceroni, A., Passerini, A., Vullo, A. and Frasconi, P. (2006) DISULFIND: a disulfide bonding state and cysteine connectivity prediction server. Nucleic Acids Res. 34, W177–W181.
[24] Desikan, R., A-H-Mackerness, S., Hancock, J.T. and Neill, S.J. (2001) Regulation of the Arabidopsis transcriptome by oxidative stress. Plant Physiol. 127, 159–172.
[25] Dietz, K.J. and Pfannschmidt, T. (2011) Novel regulators in photosynthetic redox control of plant metabolism and gene expression. Plant Physiol. 155, 1477–1485.
[26] Dietz, K.J. (2014) Redox regulation of transcription factors in plant stress acclimation and development. Antioxid. Redox Signal. 21, 1356–1372.
[27] Chan-Schaminet, K.Y., Baniwal, S.K., Bublak, D., Nover, L. and Scharf, K.D. (2009) Specific interaction between tomato HsfA1 and HsfA2 creates hetero-oligomeric superactivator complexes for synergistic activation of heat stress gene expression. J. Biol. Chem. 284, 20848–20857.
[28] Sorokin, A.V., Kim, E.R. and Ovchinnikov, L.P. (2007) Nucleocytoplasmic transport of proteins. Biochemistry (Mosc) 72, 1439–1457.
[29] Jung, H.S., Crisp, P.A., Estavillo, G.M., Cole, B., Hong, F., Mockler, T.C., et al. (2013) Subset of heat-shock transcription factors required for the early response of Arabidopsis to excess light. Proc. Natl. Acad. Sci. U.S.A. 110, 14474–14479.
[30] Pérez-Salamó, I., Papdi, C., Rigó, G., Zsigmond, L., Vilela, B., Lumbreras, V., Nagy, I., Horváth, B., Domoki, M., Darula, Z., Medzihradszky, K., Bögre, L., Koncz, C. and Szabados, L. (2014) The heat shock factor A4A confers salt tolerance and is regulated by oxidative stress and the mitogen-activated protein kinases MPK3 and MPK6. Plant Physiol. 165 (1), 319–334.